Наносистеми, наноматеріали, нанотехнології
Nanosistemi, Nanomateriali, Nanotehnologii
2024, т. 22, № 2, сс. 323–334
https://doi.org/10.15407/nnn.22.02.323

© 2024 ІМФ (Інститут металофізики
ім. Г. В. Курдюмова НАН України)
Надруковано в Україні.

PACS numbers: 61.05.cp, 78.30.Hv, 78.40.Ha, 81.07.Nb, 81.16.Hc, 81.20.Fw, 81.70.Pg

Preparation of MFe$_2$O$_4$ (M Ca, Mg) Nanoparticles by Sol–Gel Method and Studying of Their Catalytic Activity

Mahmoud Alsaleh and Ibraheem Asaad Ismaeel

Department of Chemistry,
Albaath University,
Damascus–Aleppo Highway
Homs, Syria

In this paper, MFe$_2$O$_4$ nanoparticles (M = Ca, Mg) are synthesized by sol–gel method using different stabilizer (acetic acid, pectin and β-carrageenan). The stability of the formed gel is studied extensively by determining the affective conditions (type of stabilizer, molar ratio of stabiliser:M(OH)$_2$:Fe(OH)$_3$, time, and temperature) on the preparation process. The most stabilized gel obtained using β-carrageenan for both Ca, Mg with ($1.2{\cdot}10^{-2}$:1:2), ($1.37{\cdot}10^{-2}$:1:2) molar ratios, respectively, during 72 h at 25°C. The obtained gel is calcinated and analysed using DTA, XRD and IR spectroscopy. The results show that the calcium ferrite is formed at 493.2°C by orthorhombic lattice cell with particle size of 13.01 nm and the magnesium ferrite is formed at 621.4°C by cubic crystal phase with particle size of 15.93 nm.

У цій роботі наночастинки MFe$_2$O$_4$ (M = Ca, Mg) синтезовано золь–ґель-методом з використанням різних стабілізаторів (оцтова кислота, пектин і β-карраґінан). Стабільність утвореного ґелю широко вивчається шляхом визначення умов, що впливають на процес приготування (тип стабілізатора, молярне співвідношення стабілізатор:M(OH)$_2$:Fe(OH)$_3$, час і температура). Найбільш стабілізований ґель одержано з використанням β-карраґінану для обох Ca, Mg з молярними співвідношеннями ($1{,}2{\cdot}10^{-2}$:1:2), ($1{,}37{\cdot}10^{-2}$:1:2) відповідно протягом 72 годин за температури у 25°C. Одержаний ґель прожарюють і аналізують за допомогою ДТА, рентґенівської дифракції й ІЧ-спектроскопії. Результати показують, що ферит Кальцію утворюється за 493,2°C із орторомбічною коміркою ґратниці з розміром частинок у 13,01 нм, а ферит Маґнію утворюється за 621,4°C із кубічною кристалічною фазою з розміром частинок у 15,93 нм.

Key words: sol–gel method, β-carrageenan, calcium ferrite, magnesium ferrite.

Ключові слова: золь–ґель-метод, β-карраґінан, ферит Кальцію, ферит Маґнію.

(Received 3 August, 2023)

1. INTRODUCTION

Magnetic nanoparticles have been primarily used in a range of purposes such as in magnetic fluids [1], catalysis [2], and medical applications [3]. The magnetic characteristics of metal nanoparticles (NPs) is based on their frame and dimension [4]. At present, magnetic oxide nanoparticles are charming and are of considerable interest due to their wide range of applications, ranging from primary research to industrial purpose [5].

One of the many types of nanoparticles that are presently earning much attention are the $CaFe_2O_4$, $MgFe_2O_4$ NPs due to their magical catalytic, optical, and magnetic particulars [6, 7]. Chemical stability and biocompatibility are other characteristics that make these particles potentially useful for a broad range of applications [8]. $CaFe_2O_4$, $MgFe_2O_4$ compounds have been recognized for potential usage in optical and magnetic memory instruments, photovoltaic cells and gas sensors, while other applications that have been studied earlier include: the production of steel [9–12], high temperature sensors; gas absorbers; oxidation catalysts; and various other applications [13, 14]. The structure of calcium ferrite is stable in a wide temperature range [15–17]. Several methods can be used to synthesize spinal magnetic nanoparticles, such as the hydrothermal [18], ball-milling [19] coprecipitation [20], aerosolization methods [21], auto-combustion [22] and sol–gel processing.

The sol–gel method has much considerable advantages for preparation of fine particle with micro- and nanosize distribution, such as good stoichiometric leading and short processing time with lower temperature [23–26]. This work aims to preparation of the $CaFe_2O_4$, $MgFe_2O_4$ nanoparticles using sol–gel method and studying the impact of preparation parameters on gel stabilizing, and studying of the prepared compounds as catalysis for methylene blue (MB) oxidation.

2. MATERIALS AND METHODS

2.1. Materials

($Ca(NO_3)_2$ 99%), ($Mg(NO_3)2.6H_2O$ 99.5%), ($Fe(NO_3)3.9H_2O$ 99.5%) (NH_4OH 25%), (CH_3COOH 99%) were supplied from Riedel deHaen. (β-carrageenan 99.5%), (pectin 99.5%) from ChemLab. These chemicals were utilized in the synthesis of the samples using distilled water.

2.2. Sample Preparation

Calcium hydroxide and ferric hydroxide were prepared separately using NH_4OH, after that we mixed $Ca(OH)_2$ with $Fe(OH)_3$ by 1:2 molar ratio and homogenized in distilled water by stirring continuously with a magnetic stirrer for 24 h at 25°C.

To study the effect of stabilizer on the gel formation, we add different stabilizers (acetic acid, pectin and β-carrageenan) at specific conditions (molar ratio, time and temperature). After that, the formed gel was calcinated after filtration and washing with distilled water.

The previous procedure repeated for magnesium hydroxide.

2.3. Characterization of $CaFe_2O_4$, $MgFe_2O_4$ NPs

The thermal activity of fresh formed gel determined using DTA (Shimadzu), the crystallite structure and size of the synthesized nanoparticle samples were calculated using an X-Ray Powder Diffractometer (XRD) (Philips-PW-1840) with a CuK_α radiation (1.5418 Å) in a 2θ range of 20–80°, while the analysis of the chemical composition was carried out using Fourier-transformation infrared (FTIR model: Jasco Spectrum 4100 FT-IR) spectroscopy.

2.4. Catalytic Degradation Experiments

The degradation experiments were performed in the glass bottle (250 mL) containing 100 mL of MB solution. In details, a certain amount of catalyst (0.1 g) was added to the MB solution (64 mg/L) under stirring for 1 h in the dark. 10 mL of H_2O_2 solution (30% v/v) was added.

The ultraviolet–visible (UV–Vis) absorbance of supernatant was determined at wavelength of 665 nm (for MB). The catalytic activity (Ca, %) of MB was calculated by Eq. (1):

$$Ca = \frac{A_0 - A_e}{A_0} \cdot 100\%, \quad (1)$$

where A_0 and A_e are the initial and equilibrium absorptions of MB, respectively.

3. RESULTS AND DISCUSSION

3.1. Effect of Stabilizers on the Gel-Solution Stability

This experiment aims to detecting the best stabilizer for gel for-

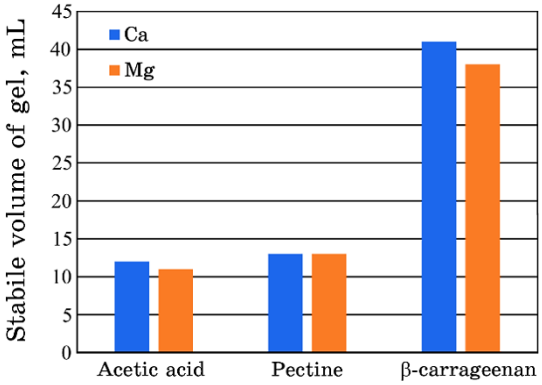

Fig. 1. The effect of the stabilizer type on the stability of the $M(OH)_2$–$Fe(OH)_3$ (M = Ca, Mg) system.

mation by comparing the stabile volume of formed gel using three different stabilizers (acetic acid, pectin and β-carrageenan), which were added with same molar ratio to the homogenized hydroxide mixture, mixed very well until full homogenous, and transferred to volumetric cylinder with notice to fixing the volume of mixture at 100 mL for all. We measured the stabile volume of gel after three days (final stabilization). Figure 1 viewing the obtained results.

As can be seen, the best stabilizer was β-carrageenan that belongs to the chemical formula. There are several hydroxyl groups, which are able to form hydrogen bonds with metal hydroxides and, thus, link these hydroxides with each other; this one prevents the precipitation of hydroxides, and thus, gives high stability to the mixture.

3.2. Effect of Stabilizer Amount on the Gel-Solution Stability

To determine the best quantity of stabilizer (β-carrageenan) on the stability of gel, different amount of (β-carrageenan) were added to the metals hydroxide mixture ranged $0.344 \cdot 10^{-2}$–$1.72 \cdot 10^{-2}$ mole. The obtained results are represented graphically in Fig. 2.

From the results, it can be noticed that, with increasing the amount of stabilizer, the stability of the gel increases (direct proportion) until reaching to the equilibrium state, which takes $1.2 \cdot 10^{-2}$ mole of stabilizer for calcium and $1.37 \cdot 10^{-2}$ mole for magnesium.

3.3. Effect of Temperature on the Gel-Solution Stability

Depending on the previous optimal conditions, the effect of temper-

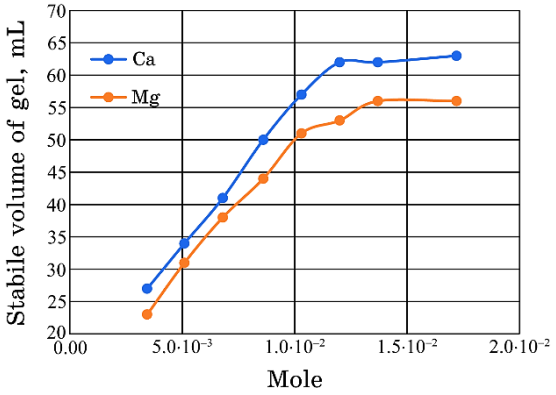

Fig. 2. The effect of the stabilizer amount on the stability of the $M(OH)_2$–$Fe(OH)_3$ (M = Ca, Mg) system.

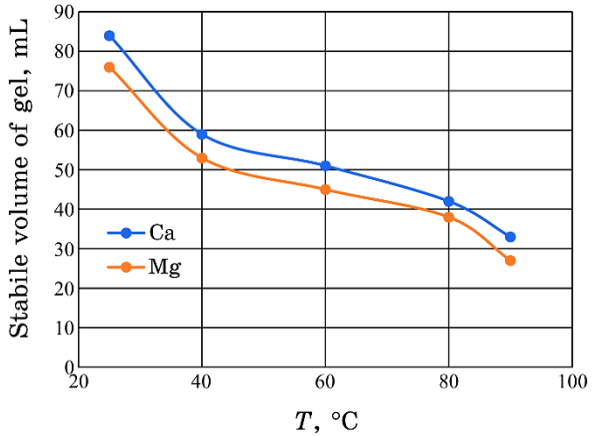

Fig. 3. The effect of the temperature on the stability of the $M(OH)_2$–$Fe(OH)_3$ (M = Ca, Mg) system.

ature on the stability of the gel formed was studied by placing the mixture in a water bath at temperatures ranging between 25–90°C.

Figure 3 shows the effect of temperature on the stability of the gel.

It is noted from the previous curve that the increase in temperature leads to a decrease in the stability of the gel and its agglomeration and its transformation into a dense precipitate. The reason for this is the increase in the thermal movement of the particles with an increase in temperature, which leads to an increase in the possibility of collisions between them and their adhesion with each other; so, they turn into large particles and precipitate in the solution.

3.4. Effect of Aging Time on the Gel Stability

The stability of the formed gel was studied over time. Figure 4 shows the obtained results. We notice a decrease in the stability of the system over time until the stability state. The reason for the decrease in the stability of the system is due to the increase in time because of the effect of gravity that leads to the compression of the formed gel and its gathering at the bottom. After 72 h, we note the stability of the gel volume and the stability of the system.

3.5. DTA Analysis

Figure 5 shows the thermal behaviour of the $M(OH)_2$–$Fe(OH)_3$

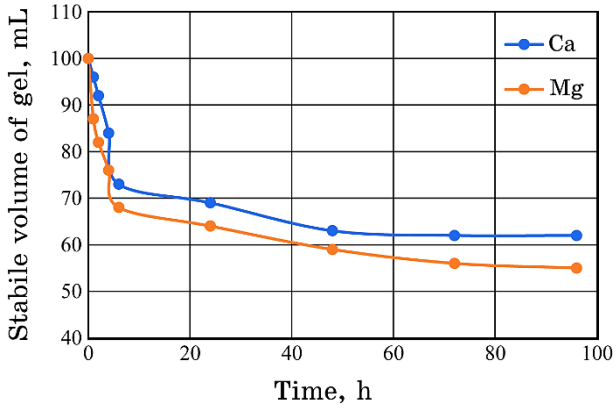

Fig. 4. The effect of the ageing time on the stability of the $M(OH)_2$–$Fe(OH)_3$ (M = Ca, Mg) system.

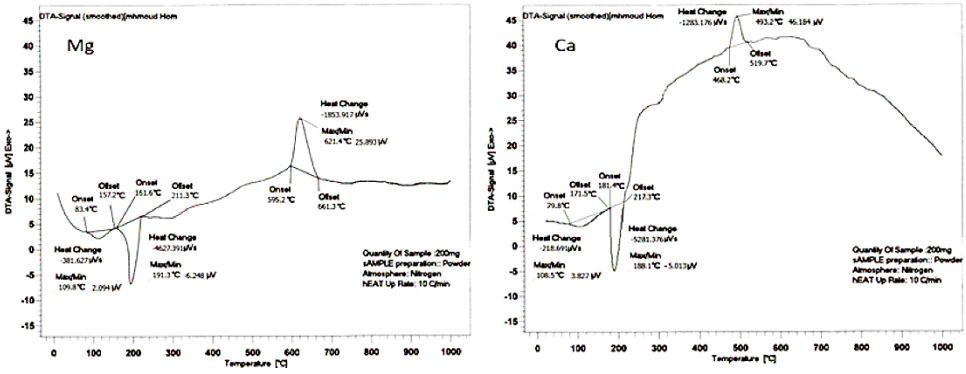

Fig. 5. DTA behaviour of the $M(OH)_2$–$Fe(OH)_3$ (M = Ca, Mg) system.

(M = Ca, Mg) system compounds, as it was scanned within a range of temperatures 0–1000°C. The thermal analysis chart (DTA) of the prepared sample shows endothermic effects and a heat dissipative effect. The first thermal effect takes place at the temperature 108.5°C (109.8°C) and refers to the physical dehydration by the samples. The second effect is also endothermic and indicates the decomposition of the used stabilizer at a temperature of 188.1°C (191.3°C), while the third effect is exothermic and takes place at 493.2°C (621.4°C) and indicates the beginning of the formation of the spinal calcium ferrite $CaFe_2O_4$ (magnesium ferrite $MgFe_2O_4$).

3.6. XRD Analysis

The XRD patterns for the prepared $CaFe_2O_4$, $MgFe_2O_4$ nanoparticles *via* sol–gel method are shown in Fig. 6. The phase of the samples was that of an orthorhombic structure for $CaFe_2O_4$, and cubic for $MgFe_2O_4$.

The calculated unit cell parameters, $a = 8.3824$ Å, $b = 8.3619$ Å, $c = 9.5567$ Å for $CaFe_2O_4$ and $a = 8.36$ Å for $MgFe_2O_4$, in tow patterns are in a good agreement with the values reported in the JCPDS file #96-901-3282 for $CaFe_2O_4$, JCPDS file #96-101-1242 for $MgFe_2O_4$. Figure 7 shows the lattice cells of prepared metal fer-

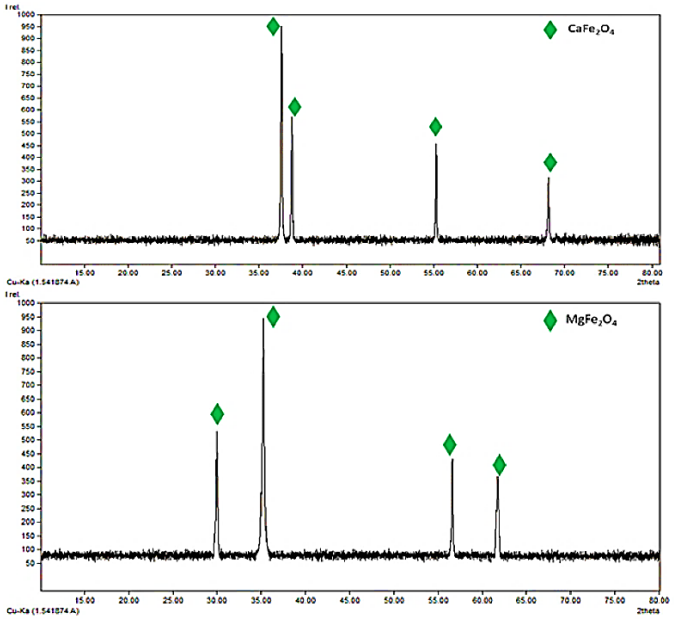

Fig. 6. XRD patterns of $CaFe_2O_4$, $MgFe_2O_4$ NPs.

rite.

The average crystallite size was calculated using Scherrer's equation, which is expressed as follows [27, 28]:

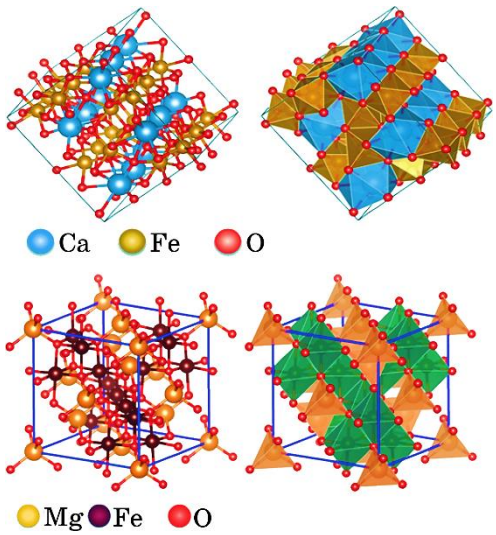

Fig. 7. Lattice cells of $CaFe_2O_4$, $MgFe_2O_4$ NPs.

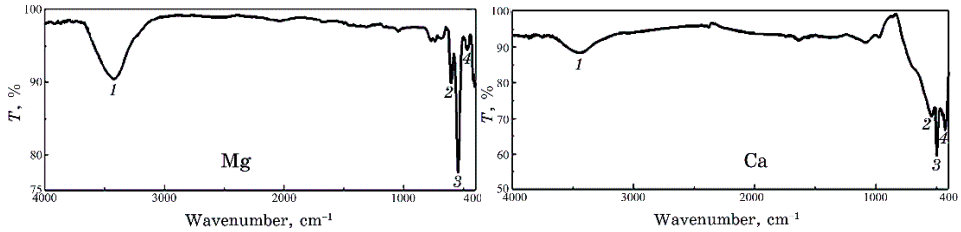

Fig. 8. FTIR spectra of synthesized CaF_2O_4, $MgFe_2O_4$ NPs.

TABLE 1. The absorption-bands' wave number of the FTIR spectra of CaF_2O_4, $MgFe_2O_4$ NPs.

Ca		Mg	
Wave number, cm^{-1}	Bond type	Wave number cm^{-1}	Bond type
3442	O–H (stretching)	3423	O–H (stretching)
652	Ca–O (as stretching)	613	Mg–O (as stretching)
502	Ca–O–Fe (as stretching)	551	Mg–O–Fe (as stretching)
434	Fe–O (as stretching)	474	Fe–O (as stretching)

$$D = \frac{K\lambda}{\beta \cos\theta}, \quad (2)$$

where K is Scherrer's constant ($K = 0.89$ assuming spherical particles), λ is the x-ray wavelength, β is the peak width at half-maximum $FWHM$, and θ is the Bragg's diffraction angle. The average crystal size was of 13.01 nm for $CaFe_2O_4$ and of 15.93 nm for $MgFe_2O_4$.

3.7. FTIR Analysis

The FTIR spectra of CaF_2O_4, $MgFe_2O_4$ nanoparticles are presented in Fig. 8. All the FTIR spectra results, which were observed in the range of 4000–000 cm^{-1} at room temperature, are arranged in Table 1. The most important absorption bands in the spectra are at 502 cm^{-1}, 551 cm^{-1}, which belong to Ca–O–Fe, Mg–O–Fe, respectively, that confirms the formation of CaF_2O_4, $MgFe_2O_4$.

3.8. The Catalytic Activity

The catalytic activity of CaF_2O_4, $MgFe_2O_4$ NPs prepared by the sol–gel method was studied through the methylene blue oxidation reaction using hydrogen peroxide. Figure 9 shows the absorption spectra of methylene blue in the presence of different catalysis after 1 h of reaction time. The catalytic activity was calculated through Eq. (1). The obtained results are arranged in Table 2.

As can be seen from the previous results, the largest reached catalytic activity was in the presence of $CaFe_2O_4$, which has a particles' size smaller than the $MgFe_2O_4$-particles' size.

4. CONCLUSION

$CaFe_2O_4$, $MgFe_2O_4$ NPs were successfully synthesized using sol–gel method. The effect of several factors on the stability of the formed gel (type of stabilizer, quantity and temperature) was also studied. The resulting compounds were characterized using XRD techniques, which confirmed the size of nanoparticles, and IR spectroscopy. The catalytic activity was studied, and it was found that the most effective compound is $CaFe_2O_4$.

5. HIGHLIGHTS:

Synthesis of calcium and magnesium ferrite nanoparticles; charac-

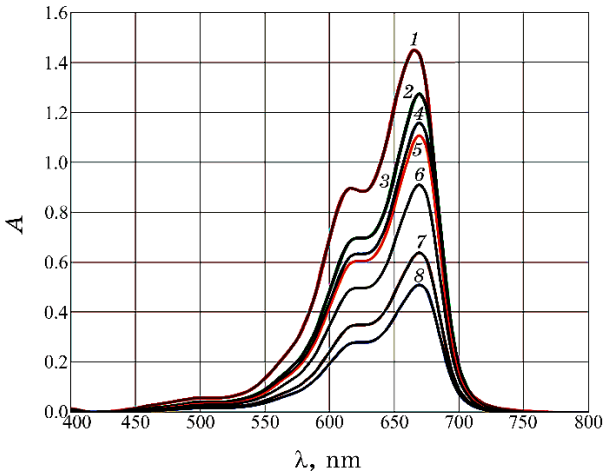

Fig. 9. UV–Vis spectra of MB in the presence of different catalysis.

TABLE 2. Catalytic activity for MB oxidation reaction in the presence of different catalysts.

Catalyst	CaO	MgO	Fe_2O_3	$CaFe_2O_4$	$MgFe_2O_4$
Ca (%)	13.043	9.901	28.571	60	50.001

terization of the prepared compounds; studying the catalytic activity of the prepared compounds by the oxidation of methylene blue.

REFERENCES

1. R. Taylor, S. Coulombe, T. Otanicar, P. Phelan, A. Gunawan, W. Lv, G. Rosengarten, R. Prasher, and H. Tyagi, *Journal of Applied Physics*, **113**, Iss. 1: 011301 (2013); https://doi.org/10.1063/1.4754271
2. S. F. Wang, X. T. Zu, G. Z. Sun, D. M. Li, C. D. He, X. Xiang, W. Liu, S. B. Han, and S. Li, *Ceramics International*, **42**, Iss. 16: 19133 (2016); https://doi.org/10.1016/j.ceramint.2016.09.075
3. T. Zargar and A. Kermanpur, *Ceramics International*, **43**, Iss. 7: 5794 (2017); https://doi.org/10.1016/j.ceramint.2017.01.127
4. A. Abedini, A. Rajabi, F. Larki, M. Saraji, and M. S. Islam, *Journal of Alloys and Compounds*, **711**: 190 (2017); https://doi.org/10.1016/j.jallcom.2017.03.356
5. M. Goodarz Naseri, E. B. Saion, and A. Kamali, *International Scholarly Research Notices*, **2012**: 1 (2012); https://doi.org/10.5402/2012/604241
6. Sh. Ida, K. Yamada, T. Matsunaga, H. Hagiwara, Ya. Matsumoto, and T. Ishihara, *Journal of the American Chemical Society*, **132**, Iss. 49: 17343 (2010); https://doi.org/10.1021/ja106930f
7. S. K. Pardeshi and R. Y. Pawar, *Materials Research Bulletin*, **45**, Iss. 5: 609

(2010); https://doi.org/10.1016/j.materresbull.2010.01.011
8. R. A. Candeia, M. I. B. Bernardi, E. Longo, I. M. G. Santos, and A. G. Souza, *Materials Letters*, **58**, Iss. 5: 569 (2004); https://doi.org/10.1016/S0167-577X(03)00563-9
9. M. Dadwal, D. Solan, and H. Pradesh, *Journal of Advanced Pharmacy Education & Research*, **4**, Iss. 1: 20 (2014).
10. R. J. Willey, P. Noirclerc, and G. Busca, *Chemical Engineering Communications*, **123**, Iss. 1: 1 (1993); https://doi.org/10.1080/00986449308936161
11. L. G. J. de Haart and G. Blasse, *Journal of the Electrochemical Society*, **132**, Iss. 12: 2933 (1985); https://doi.org/10.1149/1.2113696
12. Y. Huang, Y. Tang, J. Wang, and Q. Chen, *Materials Chemistry and Physics*, **97**, Iss. 2–3: 394 (2006); https://doi.org/10.1016/j.matchemphys.2005.08.035
13. D. Hirabayashi, T. Yoshikawa, K. Mochizuki, K. Suzuki, and Y. Sakai, *Catalysis Letters*, **110**: 155 (2006); https://doi.org/10.1007/s10562-006-0104-0
14. N.O. Ikenaga, Y. Ohgaito, and T. Suzuki, *Energy & Fuels*, **19**, Iss. 1: 170 (2005); https://doi.org/10.1021/ef049907z
15. V. V. Kharton, E. V. Tsipis, V. A. Kolotygin, M. Avdeev, A. P. Viskup, J. C. Waerenborgh, and J. R. Frade, *Journal of the Electrochemical Society*, **155**, Iss. 3: 13 (2008); https://doi.org/10.1149/1.2823458.
16. C. Ling and F. Mizuno, *Chemistry of Materials*, **25**, Iss. 15: 3062 (2013); https://doi.org/10.1021/cm401250c
17. B. Phillips and A. Muan, *Journal of the American Ceramic Society*, **41**, Iss. 11: 445 (1958); https://doi.org/10.1111/j.1151-2916.1958.tb12893.x
18. J. Wan, X. Chen, Z. Wang, X. Yang, and Y. Qian, *Journal of Crystal Growth*, **276**, Iss. 3–4: 571 (2005); https://doi.org/10.1016/j.jcrysgro.2004.11.423
19. S. K. Pradhan, S. Bid, M. Gateshki, and V. Petkov, *Materials Chemistry and Physics*, **93**, Iss. 1: 224 (2005); https://doi.org/10.1016/j.matchemphys.2005.03.017
20. Z. Yuanbi, Q. Zumin, and J. Huang, *Chinese Journal of Chemical Engineering*, **16**, Iss. 3: 451 (2008); https://doi.org/10.1016/S1004-9541(08)60104-4
21. E. Ruiz-Hernández, A. López-Noriega, D. Arcos, I. Izquierdo-Barba, O. Terasaki, and M. Vallet-Regí, *Chemistry of Materials*, **19**, Iss. 14: 3455 (2007); https://doi.org/10.1021/cm0705789
22. M. Faraji, Y. Yamini, and M. Rezaee, *Journal of the Iranian Chemical Society*, **7**: 1 (2010); https://doi.org/10.1007/BF03245856
23. A. Pradeep and G. Chandrasekaran, *Materials Letters*, **60**, Iss. 3: 371 (2006); https://doi.org/10.1016/j.matlet.2005.08.053
24. Z. Yue, J. Zhou, L. Li, H. Zhang, and Z. Gui, *Journal of Magnetism and Magnetic Materials*, **208**, Iss. 1–2: 55 (2000); https://doi.org/10.1016/S0304-8853(99)00566-1
25. Z. Yue, W. Guo, J. Zhou, Z. Gui, and L. Li, *Journal of Magnetism and Magnetic Materials*, **270**, Iss. 1–2: 216 (2004); https://doi.org/10.1016/j.jmmm.2003.08.025
26. H. Spiers, I. P. Parkin, Q. A. Pankhurst, L. Affleck, M. Green, D. J. Caruana, M. V. Kuznetsov, J. Yao, G. Vaughan, A. Terry, and A. Kvick, *Journal of Materials Chemistry*, **14**, Iss. 7: 1104 (2004); https://doi.org/10.1039/B314159B

27. J. Cao, W. Chen, L. Chen, X. Sun, and H. Guo, *Ceramics International*, **42**, Iss. 15: 17834 (2016); https://doi.org/10.1016/j.ceramint.2016.08.114
28. N. Zanganeh, S. Zanganeh, A. Rajabi, M. Allahkarami, R. Rahbari Ghahnavyeh, A. Moghaddas, M. Aieneravaie, N. Asadizanjani, and S. K. Sadrnezhaad, *Journal of Coordination Chemistry*, **67**, Iss. 3: 555 (2014); https://doi.org/10.1080/00958972.2014.892590